A Parrinello–Rahman approach to vortex lattices

R. Carretero-González [a,*], P.G. Kevrekidis [b], I.G. Kevrekidis [c],
D. Maroudas [d], D.J. Frantzeskakis [e]

[a] *Nonlinear Dynamical Systems Group, Department of Mathematics and Statistics, San Diego State University,
San Diego, CA 92182-7720, USA*
[b] *Department of Mathematics and Statistics, University of Massachusetts, Amherst, MA 01003-4515, USA*
[c] *Department of Chemical Engineering and PACM, Princeton University, 6 Olden Str., Princeton, NJ 08544, USA*
[d] *Department of Chemical Engineering, University of Massachusetts, Amherst, MA 01003-3110, USA*
[e] *Department of Physics, University of Athens, Panepistimiopolis, Zografos, Athens 15784, Greece*

Abstract

We present a framework for studying vortex lattice patterns and their structural transitions, using the Parrinello–Rahman (PR) method for molecular-dynamics (MD) simulations. Assuming an interaction between vortices derived from a Ginzburg–Landau field-theoretic context, we extract the ground-state of a "vortex gas" using the PR-MD technique and find it to be a triangular pattern. Other patterns are also obtained for special initial conditions. Generalizations of the technique, such as the inclusion of external potentials or excitation of quadrupolar modes, are also commented upon.
© 2005 Elsevier B.V. All rights reserved.

Keywords: Vortices; Molecular dynamics; Parrinello–Rahman; Vortex lattices; Bose–Einstein condensation

1. Introduction

The study of configurations and dynamics for a large number of topological charges has gained considerable momentum due to the recent experimental advances in creating vortices [1] and vortex lattices [2–5] in Bose–Einstein condensates (BECs) [6,7]. Vortex lattices (VLs) [2–5] are particularly intriguing for many reasons. They are observed to be much more robust experimentally than was expected theoretically [8]. Also, they form very clearly ordered triangular lattices under the considered experimental conditions [2]. These are the so-called Abrikosov lattices [9], that were predicted long before in the theory of superconductivity. In the context of type-II super-

* Corresponding author.
  E-mail address: carreter@sciences.sdsu.edu
(R. Carretero-González).
  URL: http://nlds.sdsu.edu/.

conductors, the free energy arguments of Ref. [10] can be used to demonstrate that the triangular lattice is the most energetically favorable, ground-state[1] configuration. Experimental images of such lattices can be found in Ref. [11]. Furthermore, these lattices can be distorted and may display interesting non-equilibrium dynamics, upon excitation of appropriate quadrupolar modes forming transient orthorhombic, sheetlike or other patterns such as ones containing dislocation defects and other types of "imperfections" in their crystalline structure [2,3].

Naturally, such patterns of topologically charged states in the context of BECs have rejuvenated the interest in the study of vortices (see, e.g., Ref. [12] for a recent review) and more specifically in the study of lattices (see, e.g., Refs. [13,14] and references therein). We mention in passing that such patterns are also relevant in a variety of other contexts including superfluid ^{3}He [15], as well as fluid mechanics (see, e.g., Ref. [16]). Motivated by these findings, we revisit the topic of vortex lattices where we will assume, to first-order approximation, that the vortex "particles", initialized at random locations and without kinetic energy in this setting, do not feel any external parabolic potential (below we relax this assumption).

Our aim is to provide a proof-of-principle example of how to implement, in the vortex lattice context, the Parrinello–Rahman (PR) technique that has been successfully used in the study of ground states and stress-induced structural transitions of crystalline materials [17]. The original idea of Parrinello and Rahman was to develop a molecular-dynamics (MD) extended-system method [18] that accounts for box shape and size changes, i.e., the shape and size of the computational domain (box) in which the dynamics occurs are themselves properly treated as dynamical variables. In Ref. [17], this allows to exert an external isotropic stress and observe structural phase transitions. In our setting, this allows a given pattern to transfer some of its energy to the "flexible" domain, and hence assume (or modify) its own ground-state configuration. To this date, this has been a widely used

technique in the MD context (see, e.g., Refs. [19–21] and references therein for variants of the method).

The main theme of this contribution is to present systematically the PR-MD approach for vortex lattices based on a quasi-particle approach that incorporates pairwise potential interactions. We will implement the PR-MD technique to obtain the triangular ground-state configuration, as well as other metastable, transient states for a pairwise potential derived from the interaction of spirals in the context of the complex Ginzburg–Landau equation. Finally, we will discuss how the technique can be extended to account for external potentials or to illustrate structural transitions of the VLs. By using this PR-MD approach it is possible to follow *large* (infinite) clouds of vortices, their crystalline configurations and structural transitions, without the need of numerically solving the original field-theoretic models. This in turn allows for a systematic study of possible structural transitions and their excitations (using coarse computational techniques, see conclusions) that otherwise would be prohibitive using the original field-theoretic settings.

2. PR-MD general setting

The PR-MD technique is based on *augmenting* the vortex dynamical equations in a systematic fashion with equations for the *MD cell* (box) in which the vortices are contained [17]. Here, we adapt the PR-MD approach to the two-dimensional setting relevant to vortices. If we assume that the coordinates of the base vectors $(\vec{a}, \vec{b})^T$ are $(a_x, a_y)^T$ and $(b_x, b_y)^T$, respectively (T denotes transpose), then these form a 2×2 matrix, denoted $\mathbf{h}$ in the PR notation, with $h_{11} = a_x$, $h_{21} = a_y$, $h_{12} = b_x$ and $h_{22} = b_y$. Then, the metric matrix $\mathbf{G} = \mathbf{h}^T \mathbf{h}$ can also be identified as a simple (symmetric) 2×2 matrix. Using then the PR ansatz [17], one writes down the Lagrangian for the augmented dynamics as:

$$\mathcal{L} = \frac{1}{2} \sum_n M \big(G_{11} \dot{\xi}_n^2 + 2 G_{12} \dot{\xi}_n \dot{v}_n + G_{22} \dot{v}_n^2 \big)$$
$$- p_{\text{ext}} S + \frac{1}{2} W \big(\dot{a}_x^2 + \dot{a}_y^2 + \dot{b}_x^2 + \dot{b}_y^2 \big)$$
$$- \sum_{m,n} V(r_{mn}, \psi_{mn}). \tag{1}$$

---

[1] While vortex lattice configurations are highly excited states, we use in this Letter the term *ground-state* to denote a configuration that minimizes energy within the subset of vortex lattice configurations.

In the above Lagrangian, V is the vortex–vortex pairwise interaction potential (see below). W is the "mass" of the MD cell (the dynamics is typically independent of its value; the latter determines how fast—for small W—or slowly—for large W—the dynamics will approach its long-term behavior). M is the mass of the particles. Since we are only interested in ground-state configurations the actual value of the mass is irrelevant (the ground state only depends on the potential interaction between particles). So, without loss of generality of our results we set $M = 1$. p_{ext} is the externally applied hydrostatic pressure to the MD cell. In what follows we set $p_{ext} = 0$; however, we have checked that $p_{ext} > 0$ leads to essentially the same lattice configurations with slightly smaller MD box sizes. Notice that in 3D, p_{ext} multiplies the volume Ω [17]. The 2D analog is multiplying the surface $S = |\vec{a} \times \vec{b}|$. r_{mn} is the distance between the vortex centers (x_m, y_m) and (x_n, y_n), while ψ_{mn} is determined by the angle between the centers and the horizontal (X) direction: $\psi_{mn} = \tan^{-1}[(y_m - y_n)/(x_m - x_n)]$. Notice that the physical coordinates $\vec{r}_n = (x_n, y_n)^T$ and the PR-MD (scaled computational) coordinates $\vec{s}_n = (\xi_n, \nu_n)^T$ are connected through $\vec{r}_n = \mathbf{h} \cdot \vec{s}_n$. The ensemble inherent in our formalism is an iso-enthalpic, isobaric one, but using the ideas of Ref. [17], it can be extended to an isostress and/or isothermal case. In fact, we implemented an isothermal–isobaric version of the MD approach (by rescaling the velocities of the particles) and found that the equilibrium configurations were practically indistinguishable from the isoenthalpic–isobaric ones.

From the 2D Lagrangian (1), one can obtain the dynamics for each of the $4N + 8$ degrees of freedom, say q_n and $\dot{q}_n$, via the Euler–Lagrange equations:

$$\frac{d}{dt}\frac{\partial \mathcal{L}}{\partial \dot{q}_n} = \frac{\partial \mathcal{L}}{\partial q_n}. \tag{2}$$

To derive and solve these dynamical equations, we need the interaction potential between the vortices. For our proof-of-principle example, we will use the vortex–vortex interaction potential derived by Aranson et al. [22] for spiral defects in the complex Ginzburg–Landau (CGL) equation. The motivation for this choice stems from the fact that at nonzero temperatures, dissipation should be considered (due to the depletion of atoms from the condensate and into the gas phase); then the Gross–Pitaevskii equation (GPE) [7],

used to describe the BECs at zero temperature assumes complex coefficients and hence becomes an effective CGL equation. Such a dissipative model follows the form presented in Ref. [23], where it was obtained phenomenologically to incorporate damping in BECs (see also, e.g., Ref. [24] for other superfluid systems). Nevertheless, as shown in Ref. [25], such a CGL equation may also be derived (under some approximations) from a generalized GPE describing a trapped Bose gas at finite temperature [26]. However, apart from our purpose to "emulate" situations encountered in realistic experiments, the particular form of the interaction potential is also consistent with the fact that the CGL spirals have the same essential dynamic ingredients as the vortices in the GPE: (a) opposite-charge structures travel together perpendicular to the line that joins them and (b) same-charge structures produce a force perpendicular to the line that joins them, and thus rotate around each other. Furthermore, it should be noted that the interactions of CGL defects are more complicated [22] than the standard logarithmic interaction of vortices in superfluid helium [27]. Thus, the potential used in the MD simulations is:

$$V(r, \psi) = \sqrt{\frac{\beta_1}{r}}e^{-(\beta_1 r)} - \sqrt{\frac{\beta}{r}}e^{-(\beta r + \alpha(\sigma_m + \sigma_n)\psi)}, \quad (3)$$

where σ_i is the topological charge of vortex i. The second term in (3) corresponds to a long-range attraction and is the term that arose in the CGL studies of Ref. [22]. However, notice that we also incorporate a phenomenological first term in Eq. (3) that corresponds to a short-range repulsion, justified by the nature of the vortex–vortex interaction (and the fact that the vortices do not collapse into each other, but rather rotate or propagate at a certain distance from each other). Note that the parameter α in Eq. (3) controls the rotation of the vortex cloud, while β_1 (β) measures the strength of the repulsive (attractive) force between the vortices. We should remark here that for the large class of potentials with long-range attraction and short-range repulsion, these results will essentially be model independent.

3. PR-MD ground-state simulations

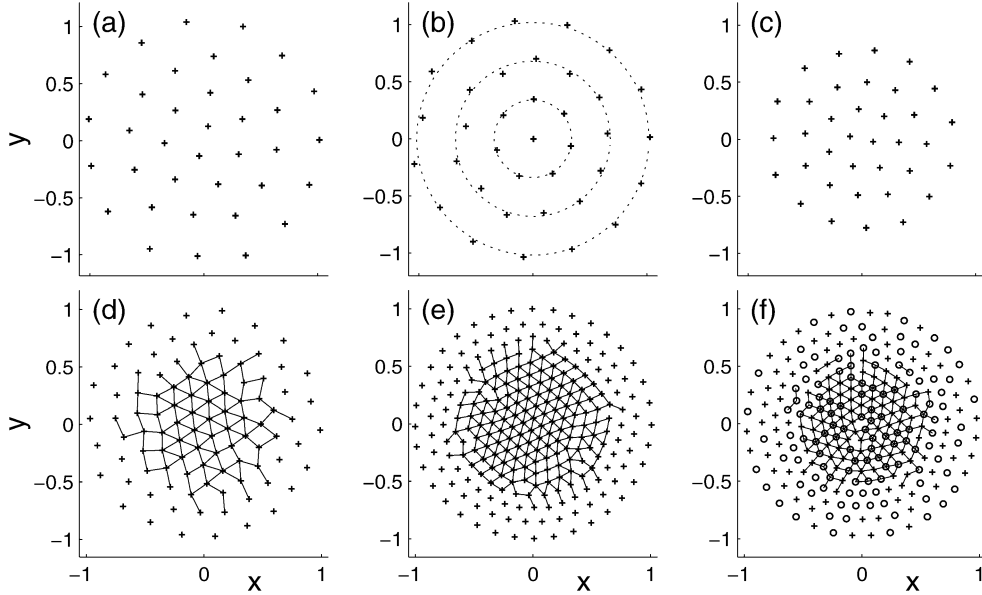Having set up the dynamical framework via Eqs. (1)–(3), we can now examine the properties of

Fig. 1. Crystalline configurations obtained from the PR-MD simulations without PBCs. The parameters are: $\beta = 1$, (a)–(c) $N_v = 36$, $\alpha = 0$; (d) $N_v = 100$; (e)–(f) $N_v = 249$; (d)–(f) $\alpha = 0.001$; (a), (b) $\beta_1 = 2$ and (c)–(f) $\beta_1 = 3.25$. For (a)–(e), all vortices have same charge and for (f) approximately half of the vortices have charge $\sigma = +1$ (crosses) and the other half $\sigma = -1$ (circles). In order to enhance the crystalline structure, thin lines are plotted connecting approximately equispaced vortices.

the vortex crystalline structure, using the PR-MD technique. Firstly, we examine the behavior for a *finite* number of vortices by performing numerical experiments in a cell without implementing periodic boundary conditions (PBCs). In Fig. 1, we present typical results from the PR-MD simulations for increasing number of vortices. Typically, for a small number of vortices ($N_v = 36$, cf. Fig. 1(a)–(c)), the crystalline configuration corresponds to patterns of equispaced concentric rings (see dotted circles in inset (b)), resembling the behavior of a shell-type model. For a larger number of vortices ($N_v > 100$), the crystalline pattern corresponds to a core with a triangular configuration surrounded by circular shells. This behavior is reminiscent of the competition between circular symmetry and the tendency towards triangular patterns in rotating superfluids [28]. The results presented in Fig. 1 tend to suggest that in the large-N_v limit the ground-state configuration is a triangular lattice pattern.

In the experimental settings (see, e.g., Refs. [2,3]), it is typically possible to generate hundreds of vortices. Hence, it is relevant to examine the behavior of a lattice consisting of many vortices (and in part to consider the thermodynamic limit of $N_v \to \infty$). To study

such configurations, we impose PBCs around the MD box and adopt the so-called minimum image convention for interactions with particles in all 8 neighboring periodic image boxes of the original cell (for each vortex only the largest N_v contributions, from all 9 boxes, are used) [18].

In order to obtain the ground-state configuration of the system, we initialize the MD simulation with a vortex cloud of same-charge vortices placed at random locations inside the box. The mean-path distance between neighboring vortices was chosen to be close to the location of the minimum of the pairwise potential (3) in order to ensure a small deformation of the box as the vortex cloud crystallizes. A typical simulation is depicted in Fig. 2, where the initial random cloud of $N_v = 225$ same-charge vortices equilibrates to a triangular configuration. The net effect of the α term in the pairwise potential (3) is to rotate the whole cloud clockwise (for positive charges). Nevertheless, the box adjusts itself to the rotation and the cloud in scaled computational coordinates (ξ, ν) appears stationary after the crystalline structure equilibrates. It is worth mentioning that, since the PR-MD Lagrangian dynamics is conservative, the obtained equilibrated
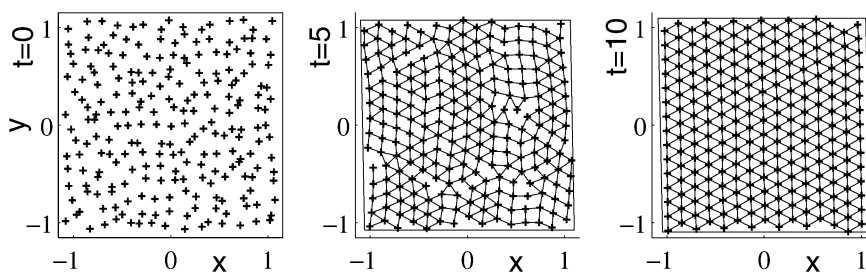
Fig. 2. MD simulation with a random initial pattern of $N_v = 225$ same-charge vortices. After a short transient ($t < 8$), the configuration equilibrates into a triangular lattice ($t = 10$). Parameters: $\alpha = 0.00001$, $\beta = 2$ and $\beta_1 = 3.25$.
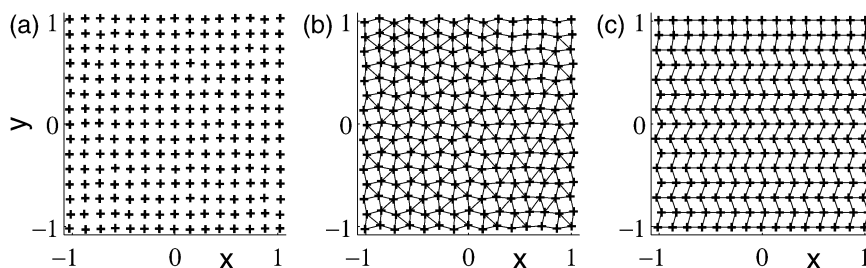

Fig. 3. MD simulations with an initial pattern (a) corresponding to a slightly perturbed square lattice of $N_v = 225$ same-charge vortices. (b) After some transient, the configuration equilibrates to a star pattern. (c) Rhomboidal pattern obtained from a slightly different initial perturbation of (a). Same parameters as in Fig. 2.

patterns have the same total energy (in computational coordinates) as the initial configuration and the "excess" energy (kinetic and potential) of the individual particles is stored by the box itself. Extensive simulations using different initial conditions and parameters typically settled into a rotating *triangular lattice*. This suggests that the ground-state configuration for a large cloud of vortices corresponds to a triangular lattice as has been observed in the BEC experiments [2]. For clarity of presentation, all the figures in this manuscript are depicted in a co-rotating reference frame in real (physical) coordinates.[2] The results presented here are not particularly sensitive to the initial state of the box (size or shape) or the position of the vortices— provided that the initial configuration, in real coordinates, is not (energetically) far from the triangular crystalline ground state. It is also possible to obtain a triangular crystalline configuration by starting with an MD box angle close to $\pi/3$ and vortices arranged

close to a square configuration in computational coordinates (i.e., a triangular configuration in real coordinates).

For some simulations, dislocation defects (and, in general, lattice imperfections) on the final configuration were clearly visible; in particular, this is observed when the number of vortices in our "unit box" is such that a uniform tiling of the plane cannot be achieved. During our MD simulations, we were able to observe some richer periodic patterns. Specifically, when starting from a slightly perturbed square lattice, the vortex cloud does not necessarily equilibrate to a triangular crystal but rather, for different initial perturbations, to a rhomboidal crystal (similar to the one observed in a BEC experiment [4]) or to a combination of local triangular and square blocks. These crystalline structures are *local* minima of the total energy—large enough perturbations destroy them and the cloud equilibrates to a triangular lattice. An example of this rich pattern formation is presented in Fig. 3 where the frozen crystalline structures corresponding to "star" and rhomboidal patterns are depicted. Such transient patterns, as well as dislocation type defects also have been observed in the experiments of Refs. [2,3].

---

[2] Notice that the rotation can be "factored out" by imposing a non-holonomic constraint; however, we did not incorporate such an approach in the present setting.
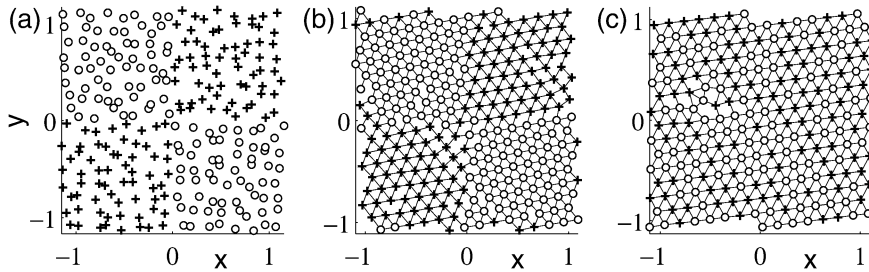
Fig. 4. MD simulation of $N_v = 256$ mixed charge vortices. Half of the vortices are set with charge $\sigma = +1$ (crosses) and placed in the first and third quadrants, while the other half are set with charge $\sigma = -1$ (circles) and placed in the remaining quadrants. (a) Initial configuration. (b) For $\alpha = 0.001$, the configuration equilibrates to a triangular lattice with no mixing of the sub-clouds of different charges. (c) For $\alpha = 0.01$, the rotation of each sub-cloud is strong enough to "mix" the initial configuration that finally settles down to a triangular lattice of well mixed positive- and negative-charge vortices.

Up to this point, we have treated cases where all the vortices have the same charge (except Fig. 1(f)). Let us briefly describe the case of a vortex cloud with mixed charges. A cloud of positively (negatively) charged vortices rotates clockwise (counter-clockwise). Fig. 4 depicts the chief characteristics for the evolution of a mixed-charge vortex cloud. The MD simulation is started with 2 positive-charge clouds (first and third quadrants) and 2 negative-charge clouds (second and fourth quadrants), for a total of $N_v = 256$ vortices. For weak rotation ($\alpha = 0.001$), each sub-cloud rapidly equilibrates to a triangular pattern (inset (b)) with some defects at the sub-cloud boundaries. However, for stronger rotation ($\alpha = 0.01$), the sub-clouds mix and finally settle to a well mixed triangular pattern (inset (c)) similar to the one depicted for a mixed-charge cloud in Fig. 1(f).

4. Conclusions and extensions

In the present work, we have demonstrated how to implement the Parrinello–Rahman molecular-dynamics scheme in order to identify ground states and structural transitions of vortex lattices. We have concluded that for sufficiently large numbers of vortices, the system settles into triangular configurations which structurally resemble to the ones observed in Bose–Einstein condensate (BECs) experiments [2], even though other configurations such as the orthorhombic ones of Ref. [3], as well as structures with defects [2,3] have also been observed.

It is interesting to point out how extensions of the PR-MD technique can be implemented to account for experimentally relevant trapping or excitation condi-

tions. In particular, external potentials such as an optical lattice potential [29] in the BEC setting can be easily incorporated in the frame of Eq. (1) by introducing an effective potential acting on the coherent structure centers [30]. Furthermore, the excitation of quadrupolar or other modes, in the spirit of the experiments of Ref. [3], can be realized by identifying steady states, such as the triangular ones, by means of Newton iterations and obtaining their eigenmodes (especially ones inducing instabilities). Preliminary results yield very interesting dynamical phenomena (such as global oscillations) and will be presented elsewhere. Finally, numerical experiments with much larger numbers (but roughly fixed density) of vortices (i.e., larger cell sizes) would be very interesting in identifying whether the results presented herein persist in the "thermodynamic limit". Such studies, using the coarse computational techniques of Ref. [31], are in progress and will be reported in future publications.

Acknowledgements

References

[1] M.R. Matthews, P. Anderson, P.C. Haljan, D.S. Hall, C.E. Wieman, E.A. Cornell, Phys. Rev. Lett. 83 (1999) 2498;

K.W. Madison, F. Chevy, W. Wohlleben, J. Dalibard, Phys. Rev. Lett. 84 (2000) 806;
S. Inouye, S. Gupta, T. Rosenband, A.P. Chikkatur, A. Görlitz, T.L. Gustavson, A.E. Leanhardt, D.E. Pritchard, W. Ketterle, Phys. Rev. Lett. 87 (2001) 080402.

[2] J.R. Abo-Shaeer, C. Raman, J.M. Vogels, W. Ketterle, Science 292 (2001) 476;
C. Raman, J.R. Abo-Shaeer, J.M. Vogels, K. Xu, W. Ketterle, Phys. Rev. Lett. 87 (2001) 210402;
J.R. Abo-Shaeer, C. Raman, W. Ketterle, Phys. Rev. Lett. 88 (2002) 070409.

[3] P.C. Haljan, I. Coddington, P. Engels, E.A. Cornell, Phys. Rev. Lett. 87 (2001) 210403.

[4] P. Engels, I. Coddington, P.C. Haljan, E.A. Cornell, Phys. Rev. Lett. 89 (2002) 100403.

[5] K.W. Madison, F. Chevy, V. Bretin, J. Dalibard, Phys. Rev. Lett. 86 (2001) 4443;
E. Hodby, G. Hechenblaikner, S.A. Hopkins, O.M. Maragò, C.J. Foot, Phys. Rev. Lett. 88 (2001) 010405.

[6] M.H. Anderson, J.R. Ensher, M.R. Matthews, C.E. Wieman, E.A. Cornell, Science 269 (1995) 198;
K.B. Davis, M.-O. Mewes, M.R. Andrews, N.J. van Druten, D.S. Durfee, D.M. Kurn, W. Ketterle, Phys. Rev. Lett. 75 (1995) 3969;
C.C. Bradley, C.A. Sackett, J.J. Tollett, R.G. Hulet, Phys. Rev. Lett. 75 (1995) 1687.

[7] F. Dalfovo, S. Giorgini, L.P. Pitaevskii, S. Stringari, Rev. Mod. Phys. 71 (1999) 463.

[8] P.O. Fedichev, A.E. Muryshev, cond-mat/0004264.

[9] A.A. Abrikosov, Sov. Phys. JETP 5 (1957) 1174.

[10] V.K. Tkachenko, Sov. Phys. JETP 22 (1966) 1282.

[11] http://cua.mit.edu/ketterle_group.

[12] A.L. Fetter, A.A. Svidzinsky, J. Phys.: Condens. Matter 13 (2001) R135.

[13] H. Aref, P.K. Newton, M.A. Stremler, T. Tokieda, D.L. Vainchtein, Vortex crystals TAM report 1008 (2002) http://www.tam.uiuc.edu/publications/.

[14] D.A. Butts, D.S. Rokshar, Nature 397 (1999) 327.

[15] T. Kita, Phys. Rev. B 66 (2002) 224515.

[16] M.D. Gunzburger, R.A. Nicolaides, Incompressible Computational Fluid Dynamics: Trends and Advances, Cambridge Univ. Press, Cambridge, 1993.

[17] M. Parrinello, A. Rahman, Phys. Rev. Lett. 45 (1980) 1196;
M. Parrinello, A. Rahman, J. Appl. Phys. 52 (1981) 7182.

[18] M.P. Allen, D.J. Tildesley, Computer Simulation of Liquids, Oxford Univ. Press, Oxford, 1990;
D.C. Rapaport, The Art of Molecular Dynamics Simulation, Cambridge Univ. Press, Cambridge, 1995.

[19] I. Souza, J.L. Martins, Phys. Rev. B 55 (1997) 8733.

[20] R. Martoňák, A. Laio, M. Parrinello, Phys. Rev. Lett. 90 (2003) 075503.

[21] J. Zhao, D. Maroudas, F. Milstein, Phys. Rev. B 62 (2000) 13799.

[22] I.S. Aranson, L. Kramer, A. Weber, Physica D 53 (1991) 376.

[23] S. Choi, S.A. Morgan, K. Burnett, Phys. Rev. A 57 (1998) 4057.

[24] I. Aranson, V. Steinberg, Phys. Rev. B 54 (1996) 13072.

[25] K. Kasamatsu, M. Tsubota, M. Ueda, Phys. Rev. A 67 (2003) 033610.

[26] E. Zaremba, T. Nikuni, A. Griffin, J. Low Temp. Phys. 116 (1999) 277.

[27] R.J. Donnelly, Quantized Vortices in He II, Cambridge Univ. Press, Cambridge, 1991.

[28] L.J. Campbell, R.M. Ziff, Phys. Rev. B 20 (1979) 1886.

[29] B.A. Anderson, M.A. Kasevich, Science 282 (1998) 1686;
F.S. Cataliotti, S. Burger, C. Fort, P. Maddaloni, F. Minardi, A. Trombettoni, A. Smerzi, M. Inguscio, Science 293 (2001) 843;
M. Greiner, O. Mandel, T. Esslinger, T.W. Hänsch, I. Bloch, Nature (London) 415 (2002) 39.

[30] See, e.g., Th. Busch, J.R. Anglin, Phys. Rev. Lett. 84 (2000) 2298;
G. Theocharis, D.J. Frantzeskakis, P.G. Kevrekidis, B.A. Malomed, Yu.S. Kivshar, Phys. Rev. Lett. 90 (2003) 120403.

[31] I.G. Kevrekidis, C.W. Gear, J.M. Hyman, P.G. Kevrekidis, O. Runborg, Commun. Math. Sci. 1 (2003) 715.